International Journal for Housing Science and Its Applications
Publish August 4, 2025. Volume 46, Issue 3 Pages 1565-1575

https://doi.org/10.70517/ijhsa463120

Dynamic planning and computation of grid dispatch optimization model under multi-terminal information interaction architecture

Siyang He[1], Hailin Yu[2], Shiqin Zhao[1], Zhen Li[3], Huaiyuan Wang[4,*], Zhengming Luo[5] and Yuchao Li[6]
[1] Duyun Power Supply Bureau of Guizhou Power Grid Corporation, Duyun, Guizhou, 558000, China
[2] Duyun Huishui Power Supply Bureau of Guizhou Power Grid Co., Ltd., Duyun, Guizhou, 550600, China
[3] Power Grid Planning Research Center of Guizhou Power Grid Corporation, Guiyang, Guizhou, 550000, China
[4] Duyun Guiding Power Supply Bureau of Guizhou Power Grid Co., Ltd., Duyun, Guizhou, 551300, China
[5] Duyun Power Supply Bureau of Guizhou Power Grid Corporation, Duyun, Guizhou, 558000, China
[6] Duyun Dushan Power Supply Bureau of Guizhou Power Grid Co., Ltd., Duyun, Guizhou, 558200, China
Corresponding authors: (e-mail: 17728117081@163.com).

Abstract This paper addresses the multi-objective optimization problem of grid scheduling under multi-terminal information interaction architecture, and proposes a grid scheduling optimization model based on adaptive dynamic planning under grid-connected mode. Taking operation cost and environmental cost as the core objectives, the multi-objective optimization scheduling model of microgrid under grid-connected mode is constructed. The idea of adaptive dynamic planning is introduced, and an improved iterative ADP algorithm is designed by combining neural networks. The model is verified by examples to generate a scheduling scheme that takes into account both economy and environmental protection: in 24-hour scheduling, the discounted solution operating cost is RMB 395.6, the environmental cost is RMB 216.0, and the storage charging and discharging strategy interacts with the main grid to dynamically match the loads and the fluctuation of electricity price. Comparative analysis shows that the iterative ADP algorithm reaches the optimal value at 250, 440, and 150 iterations, respectively, and the scheduling results satisfy the power balance and unit operation constraints while outperforming the traditional ADP algorithm.

Index Terms grid scheduling, multi-objective optimization, neural network, ADP algorithm

I. Introduction

In recent years the world's environmental problems have become increasingly severe, most countries in the world are implementing carbon neutrality, and accelerating the development of new energy sources such as solar energy, hydrogen energy, wind energy, etc. is the key to promote the world's energy development [1], [2]. At present, we need to actively carry out research on new power systems and accelerate the establishment of new power systems in order to improve the adjustable capacity of urban power systems and the stable operation of power grids [3], [4].

Although China's new energy has caught the fast train of large-scale and high-quality development, the inherent stochastic and unpredictable drawbacks of renewable energy output have brought great challenges to its grid operation and consumption [5]-[7]. In order to overcome the inherent drawbacks of renewable energy, energy storage systems are seen as a widely accepted solution. On the one hand, the vast majority of energy storage systems are geographically independent and can be controlled over different time scales [8], [9]. On the other hand, energy storage systems act as “mobile chargers” that can temporarily store and release power, smoothing out fluctuations in renewable energy output [10], [11]. However, although the rational configuration of the energy storage system can improve the operational performance of renewable energy and promote the friendly interaction between renewable energy and the power grid, the time-coupling characteristics of the energy storage system will increase the computational difficulty of the power system energy management [12]-[14]. Meanwhile, the emergence of highly penetrated renewable energy sources and flexible resources represented by energy storage and electric vehicles will change the original tidal current distribution [15], [16]. Bidirectional tidal currents may bring problems of overvoltage, reduced power supply reliability, and complicated relay protection adjustment, thus further complicating the calculation of power system optimal dispatch [17], [18]. At the same time, unlike the traditional thermal power unit-dominated traditional power system, the access of multiple devices such as renewable energy, energy storage, and demand response loads makes the power system optimal scheduling more complex [19], [20]. Based on this, a multi-terminal information interaction architecture is established, and by developing a hierarchical and distributed coordination mechanism adapted to it, the scheduling scheme with the highest overall interest of the cooperative alliance is formulated by taking into account the interests of all parties while safeguarding the information privacy between the subjects [21]-[23].

In this paper, we first deeply analyze the operation mode of grid-connected microgrids and construct the corresponding optimal scheduling model. Further elaborating the basic idea of dynamic planning, the ADP algorithm is integrated with neural network, and the iterative ADP algorithm is adopted to optimize the scheduling of microgrid. Simulation experiments are designed for the algorithms, the Pareto solution set is obtained by solving, and the compromise solution is selected by using the TOPSIS method. The output of each distributed power source under different objective functions is simulated to verify the effectiveness of the iterative ADP algorithm. The optimized scheduling results are visualized and analyzed to test the reasonableness of the scheduling scheme.

II. Construction of grid dispatch optimization model based on adaptive dynamic planning in grid-connected mode

With the rapid development of energy transition and smart grid, grid scheduling under the multi-terminal information interaction architecture faces the challenge of multi-objective optimization. Traditional scheduling methods are prone to "dimensional disaster" when dealing with high-dimensional state space and multi-objective co-optimization, and it is difficult to balance the economic and environmental requirements. In this paper, we propose an optimization model based on Adaptive Dynamic Programming (ADP) for the dynamic scheduling of microgrids in grid-connected mode, which effectively reduces the computational complexity by integrating neural network function approximation and multi-stage decision-making methods.

II. A. Multi-objective optimal scheduling of microgrids in grid-connected mode

II. A. 1) Objective function

Set the expression for the objective function Z as shown in equation (1):

$$Z = f_1 + f_2 \tag{1}$$

where: Z is the total cost of the microgrid system in the parallel operation mode; f_1 is the operating cost of the microgrid system in the parallel operation mode; and f_2 is the cost of protecting the environment of the microgrid system in the parallel operation mode.

(1) Microgrid operation cost function in grid-connected mode

Under the grid-connected operation model, the objective function for minimizing the operating cost of the microgrid system is as shown in Equation (2):

$$f_1 = \sum_{t=1}^{T} C_{grid}(t) + C_{MT}(t) + C_{DE}(t) + C_{bess}(t) \tag{2}$$

where: $C_{grid}(t)$ is the total cost of microgrid interaction with the main grid at time t; $C_{MT}(t)$ is the total operating cost of the microgas turbine at time t; $C_{DE}(t)$ is the total operating cost of the diesel generator at time t; $C_{bess}(t)$ is the cost of maintenance of the energy storage at time t; $P_{bess}(t)$ is the power of energy storage at time t; $P_{sell}(t)$ is the power sold by the microgrid and the large grid at time t; $P_{buy}(t)$ is the power purchased by the microgrid and the large grid at time t; $c_{buy}(t)$ is the power purchase tariff of the microgrid and the large grid at time t; $c_{sell}(t)$ is the electricity selling price between the microgrid and the big grid at t moment; $K_{bess,OM}$ is the operation and maintenance cost coefficient of energy storage.

1) The expression for the interaction cost

$$C_{grid}(t) = C_{buy}(t) + C_{sell}(t) \tag{3}$$

$$\begin{cases} C_{buy}(t) = c_{buy}(t) P_{buy}(t) \\ C_{sell}(t) = c_{sell}(t) P_{sell}(t) \end{cases} \tag{4}$$

2) Expression for the total operating cost of the micro gas turbine

$$C_{MT}(t) = C_{MT,OM}(t) + C_{MT,F}(t) \tag{5}$$

3) Expression for total operating cost of diesel generator

$$C_{DE}(t) = C_{DE,OM}(t) + C_{DE,F}(t) \tag{6}$$

4) Expression for the maintenance cost of energy storage

$$C_{bess}(t) = K_{bess,OM} \mid P_{bess}(t) \mid \tag{7}$$

(2) Microgrid protection environment cost function under the grid-connected model

Under the grid-connected operation model, the objective function for minimizing the cost of protecting the environment of the microgrid system is as shown in Eqs. (8) and (9):

$$f_2 = \sum_{t=1}^{T} C_{grid,EN}(t) + C_{MT,EN}(t) + C_{DE,EN}(t) \tag{8}$$

$$C_{grid,EN}(t) = \sum_{k=1}^{n} (C_k \gamma_{grid,k}) P_{buy}(t) \tag{9}$$

where: $C_{grid,EN}(t)$ is the pollutant treatment cost of the large power grid at the t moment; $\gamma_{grid,k}$ is the emission of k pollutants generated by the operation of the large power grid; C_k is the cost coefficient of treating k pollutants.

II. A. 2) Constraints

(1) An expression for the total power balance constraint of the system

$$P'_{PV}(t) + P'_{WT}(t) + P_{grid}(t) + P_{DE}(t) + P_{MT}(t) = P_L(t) + P_{bess}(t) \tag{10}$$

(2) Expression for the diesel generator constraint

$$\begin{cases} P_{DE}^{\min}(t) \le P_{DE}(t) \le P_{DE}^{\max}(t) \\ | P_{DE}(t) - P_{DE}(t-1) | \le r_{DE} \end{cases} \tag{11}$$

Where: $P_{DE}^{\min}(t)$ is t moment, the lower limit of diesel engine output; $P_{DE}^{\max}(t)$ is t moment, the upper limit of diesel engine output; r_{DE} is t moment, the upper limit of diesel engine climbing power.

(3) The expression of the micro gas turbine output power constraints

$$\begin{cases} P_{MT}^{\min}(t) \le P_{MT}(t) \le P_{MT}^{\max}(t) \\ | P_{MT}(t) - P_{MT}(t-1) | \le r_{MT} \end{cases} \tag{12}$$

where: $P_{MT}^{\min}(t)$ is t moment, the lower limit of micro-gas turbine power; $P_{MT}^{\max}(t)$ is t moment, the upper limit of micro-gas turbine power; r_{MT} is the upper limit of micro-gas turbine climbing power.

(4) The expression for the transmission power constraint of the contact line

$$P_{grid}^{\min}(t) \le P_{grid}(t) \le P_{grid}^{\max}(t) \tag{13}$$

where: $P_{grid}^{\min}(t)$ is the lower limit of the transmission power of the contact line at t moment; $P_{grid}^{\max}(t)$ is the upper limit of the transmission power of the contact line at t moment.

(5) Expression for the constraint of the energy storage device

$$\begin{cases} P_{bess}^{\min}(t) \le P_{bess}(t) \le P_{bess}^{\max}(t) \\ SOC^{\min}(t) \le SOC(t) \le SOC^{\max}(t) \end{cases} \tag{14}$$

where: $P_{bess}(t)$ is the power output of the energy storage device, its value is positive means power input, energy storage charging; its value is negative means power output, energy storage discharging; $P_{bess}^{\min}(t)$ is the lower limit of the power output of the energy storage device in the t moment; $P_{bess}^{\max}(t)$ is the upper limit of the power output of the energy storage device in the t moment; $SOC^{\min}(t)$ is the lower limit of the remaining capacity of the energy storage device at t moment; $SOC^{\max}(t)$ is the upper limit of the remaining capacity of the energy storage device at t moment.

II. B.Microgrid optimization model based on adaptive dynamic planning

II. B. 1) Basic Ideas of Dynamic Programming

(1) The key to the dynamic programming method is to correctly write the basic recurrence relations and appropriate boundary conditions (in short, the basic equations). To do this, the problem process must be divided into several interrelated stages, the appropriate selection of state variables and decision variables and the definition of the optimal value function, so that a large problem into a family of the same type of subproblems, and then solved one by one. That is, starting from the boundary conditions, recursive search for the optimal segment by segment, in the

solution of each sub-problem, are used in its previous sub-problems of the optimization results, in turn, the optimal solution of the last sub-problem, is the optimal solution of the whole problem.

(2) In the multi-stage decision-making process, the dynamic planning method is an optimization method that separates the current segment from future segments and combines the current and future benefits. Therefore, the selection of each segment of the decision is considered from the global perspective and is generally different from the optimal choice of the answer for that segment.

(3) In the search for the optimal strategy of the whole problem, because the initial state is known, and the decision of each segment is a function of the state of the segment, so the optimal strategy through the state of the segments can be transformed one by one to obtain, so as to determine the optimal route.

After clarifying the basic concepts and basic ideas of dynamic programming, we see that the following five points must be done when building a dynamic programming model for a real problem:

1) Divide the process of the problem into appropriate stages;

2) Selecting the state variable s_k correctly so that it both describes the evolution of the process and satisfies no posteriority;

3) Determine the decision variable u_k and the set of allowed decisions $D_k(s_k)$ for each stage;

4) Write the state transfer equation correctly;

5) Correctly write the relationship of the indicator function $V_{k,n}$, which should satisfy the following three properties:

(a) Be a quantitative function defined on the full process and all posterior subprocesses;

(b) It should be separable and satisfy the recurrence relation.

(c) The function $\Psi_k(s_k, u_k, V_{k,n})$ should be strictly monotonic with respect to the variables $V_{k+1,n}$.

The above five points are the basis for constructing a dynamic programming model, and are essential for correctly writing the basic equations of dynamic programming.

And whether the dynamic programming model of a problem is correctly given, it is centrally reflected in the proper definition of the optimal value function and correctly write the recurrence relation equation and boundary conditions. In short, the basic equations of dynamic programming should be written correctly.

According to the dynamic planning method there are reverse order solution method and sequential solution method, their basic equations of dynamic planning should be as follows:

Let the indicator function be in the form of taking the sum of the indicators of each stage, i.e.:

$$V_{k,n}(s_k, u_k, s_{k+1}, \cdots, s_{n+1}) = \Psi_k[s_k, u_k, V_{k,n}(s_{k+1}, \cdots, s_{n+1})] \tag{15}$$

where $V_j(s_j, u_j)$ denotes the indicator of the j th segment. It obviously satisfies the three properties of the indicator function. So the above equation can be written as:

$$V_{k,n} = V_k(s_k, u_k) + V_{k+1,n}[s_{k+1}, \cdots, s_{n+1}] \tag{16}$$

When the initial state is given, the strategy of the process is determined, then the indicator function is determined. Thus, the indicator function is a function of the initial state and the strategy. It can be written as $V_{k,n}[s_k, p_{k,n}(s_k)]$.

Therefore, the above recurrence relation can be written again as

$$V_{k,n}[s_k, p_{k,n}] = V_k(s_k, u_k) + V_{k+1,n}[s_{k+1}, p_{k+1,n}] \tag{17}$$

Its sub-strategy $p_{k,n}(s_k)$ can be viewed as a combination of decisions $u_k(s_k)$ and $p_{k+1,n}(s_{k+1})$. i.e.

$$p_{k,n} = \{u_k(s_k), p_{k+1,n}(s_{k+1})\} \tag{18}$$

If $p^*_{k,n}(s_k)$ is used to denote the optimal sub-strategy among all sub-strategies of the posterior sub-process with initial state s_k, the optimal value function is:

$$f_k(s_k) = V_{k,n}\left[s_k, p^*_{k,n}(s_k)\right] = \underset{p_{k,n}}{opt} V_{k,n}\left[s_k, p_{k,n}(s_k)\right] \tag{19}$$

and:

$$\begin{aligned} \underset{p_{k,n}}{opt} V_{k,n}\left(s_k, p_{k,n}\right) &= \underset{\{u_k, p_{k+1,n}\}}{opt} \left\{V_k(s_k, u_k) + V_{k+1,n}(s_{k+1}, p_{k+1,n})\right\} \\ &= \underset{u_k}{opt}\left\{u_k(s_k, u_k) + \underset{p_{k+1,n}}{opt} V_{k+1,n}\right\} \end{aligned} \tag{20}$$

But:

$$f_{k+1}(s_{k+1}) = \underset{p_{k+1,n}}{opt}\, V_{k+1,n}(s_{k+1}, p_{k+1,n}) \tag{21}$$

So:

$$f_k(s_k) = \underset{u_k \in D_k(s_k)}{opt}\, [V_k(s_k, u_k) + f_{k+1}(s_{k+1})] \quad k = n, n-1, \cdots, 1 \tag{22}$$

The boundary condition is $f_{n+1}(s_{n+1}) = 0$.

II. B. 2) Adaptive Dynamic Planning Based Grid Optimization

Dynamic programming is excellent at handling multi-stage problems, but in practice the storage and computational resources required climb rapidly with the increase of states and control variables, which causes the thorny problem of “dimensionality catastrophe”. The development of adaptive dynamic programming theory can overcome this problem. This theory simulates the performance index function and control strategy with the help of function approximation structure in dynamic planning, so that the optimal control strategy can be effectively approximated and realized, and the problem of “dimensional disaster” can be alleviated to a large extent. This approach maintains high computational efficiency and is more accurate in solving the problem.

For the above microgrid model, the state transfer equation is shown as follows:

$$SOC^k(t+1) = SOC^k(t) + \frac{\left(P_b^k(t) + P_{grid}^k(t) + U_{IL}(t)P_{IL}^k(t)\right)}{E_{b,cap}}\Delta t \tag{23}$$

The state of the microgrid system is

$$x(t) = (SOC^1(t), \cdots, SOC^k(t)) \tag{24}$$

The amount of microgrid system control is

$$u(t) = (P_b^1(t), P_{grid}^1(t), P_{IL}^1(t), P_b^2(t), P_{grid}^2(t), P_{IL}^2(t), \cdots, P_b^k(t), P_{grid}^k(t), P_{IL}^k(t)) \tag{25}$$

In adaptive dynamic programming, the cost function can be written as:

$$J(t) = \sum_{i=t}^{\infty} \gamma^{i-t} U(t) \tag{26}$$

where $U(t)$ is the t-time period utility function, γ is the discount factor, and $0 < \gamma \le 1$, in this paper $\gamma = 0.8$.

According to equation (26), it can be concluded that

$$J(t) = U(t) + \gamma J(t+1) \tag{27}$$

Assuming that $J^*(t+1)$ is known, by Bellman's principle, $J^*(t)$ can be written as

$$J^*(t) = \min_{u(t)} \left\{ U(t) + \gamma J^*(t+1) \right\} \tag{28}$$

The optimal control $u^*(t)$ can be obtained by the following equation

$$u^*(t) = \arg\min_{u(t)} \left\{ U(t) + \gamma J^*(t+1) \right\} \tag{29}$$

However, since $J^*(t+1)$ is unknown and $u^*(t)$ cannot be derived directly from Eq. (30), this paper utilizes adaptive dynamic programming to solve the optimal control problem described by Eq. (29).

Based on Eqs. (26)-(29), the utility function can be defined as:

$$U(t) = u(t) R u(t)^T \tag{30}$$

where R represents the weight matrix consisting of the unit price of energy storage charging and discharging, the unit price of power purchased from the grid, and the unit price of load interruption compensation.

ADP algorithms usually need to compute or approximate value functions or strategy functions. Neural networks, as a powerful function approximator, can be used to approximate these functions, especially when they are very complex or difficult to obtain by other means. The combination of neural networks and ADP allows for online learning and adaptation, since neural networks can continuously update their parameters to approximate the latest value function or policy function as the system runs.

In this paper, an adaptive dynamic planning algorithm is fused with a neural network. In this fusion model evaluates the system state $x(t)$ of the microgrid of the network, while its output is a cost function $\hat{J}(t)$, and denotes the weight matrix of the hidden layer of the evaluating network and the weight matrix of the hidden layer to the output layer by W_{c1} and W_{c2}, respectively. The structure of the evaluation neural network is shown in Fig. 1.

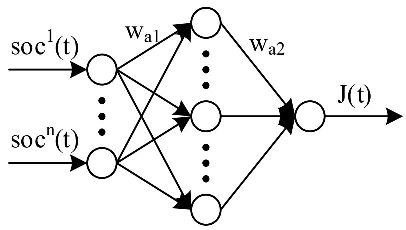

Figure 1: Evaluate neural networks

In this paper, the gradient descent method is used to train the evaluation network with the error formula expressed as follows

$$e_c(t) = \hat{J} - [\gamma \hat{J}(t+1) + U(t)] \tag{31}$$

$$E_c(t) = \frac{1}{2} e_c^2(t) \tag{32}$$

The weight matrix of the evaluation network is updated as follows

$$\Delta W_c(t) = l_c e_c(t) \left[-\frac{\partial \hat{J}(t)}{\partial W_c(t)} \right] \tag{33}$$

$$W_c(t+1) = W_c(t) + \Delta W_c(t) \tag{34}$$

where l_c is the learning rate of the evaluation network, in this paper, $l_c = 0.001$.

The input of the execution network is the system state $x(t)$, while its output is the system control $u(t)$. Where W_{a1} represents the weight matrix from the input layer to the hidden layer, and W_{a2} represents the weight matrix from the hidden layer to the output layer. The specific structure of the executive neural network is shown in Fig. 2.

The state transfer function can be written as:

$$x(t+1) = x(t) + u(t) \times C_p \tag{35}$$

where C_p is the matrix of weights associated with the system control to the system state.

The partial differential equation of the utility function with respect to the system control variables at moment t is:

$$\frac{\partial U(t)}{\partial u(t)} = 2u(t)R \tag{36}$$

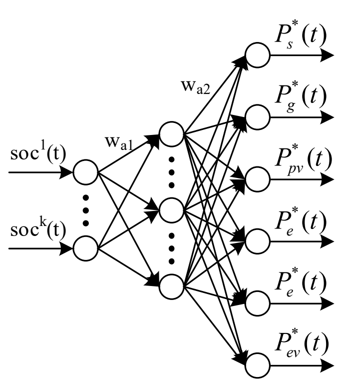

Figure 2: Execution neural network

The partial differential equation of the cost function at moment $t+1$ with respect to the control variables at moment t is

$$\frac{\partial \hat{J}(t+1)}{\partial u(t)} = \frac{\partial \hat{J}(t+1)}{\partial x(t+1)} \frac{\partial x(t+1)}{\partial u(t)} = \frac{\partial \hat{J}(t+1)}{\partial x(t+1)} C_p^T \tag{37}$$

The partial differential equation of the cost function at moment t with respect to the control variable at moment t is

$$\frac{\partial \hat{J}(t)}{\partial u(t)} = \frac{\partial \hat{J}(t+1)}{\partial u(t)} + \frac{\partial U(t)}{\partial u(t)} = \frac{\partial \hat{J}(t+1)}{\partial x(t+1)} C_p^T + 2u(t)R \tag{38}$$

According to the optimality theory, $\hat{J}(t)$ is minimized when $u(t)$ is the optimal control.

$$\left.\frac{\partial \hat{J}(t)}{\partial u(t)}\right|_{u(t)=u^*(t)} = 0 \tag{39}$$

$$u^*(t) = -\frac{1}{2} \frac{\partial \hat{J}(t+1)}{\partial x(t+1)} C_p^T R^{-1} \tag{40}$$

A gradient descent method can be used to train the execution network to minimize the error, which is expressed as

$$e_a(t) = u(t) - u^*(t) \tag{41}$$

$$E_a(t) = \frac{1}{2} e_a(t) e_a^T(t) \tag{42}$$

The implementation network weights are updated to

$$\Delta W_a(t) = l_a e_a(t) \left[-\frac{\partial u(t)}{\partial W_a(t)} \right] \tag{43}$$

$$W_a(t+1) = W_a(t) + \Delta W_a(t) \tag{44}$$

where l_a is the learning rate of the execution network, in this paper, $l_a = -0.001$.

III. Adaptive dynamic planning-based grid dispatch optimization model solution in grid-connected mode

III. A. Multi-objective optimal scheduling solution

The microgrid in this paper's algorithm contains PV, WT, battery storage, MT, and loads, and is connected to the distribution grid through a PCC. The battery storage has SOC upper and lower limits of SOCmax=0.8, SOCmin=0.3, capacity of 130kWh, charge/discharge efficiency of 0.8, and the number of scheduling time periods in a day, T, is 24 and Δt is 1, respectively.

Using the iterative ADP algorithm proposed in this paper to solve the above environmental-economic multi-objective model, the Pareto solution set obtained is shown in Fig. 3. Fig. 3 shows the Pareto frontier of the model solved by the MOPSO algorithm, with the horizontal coordinate representing the operating cost of the microgrid and the vertical coordinate representing the environmental cost incurred during the operation of this microgrid, and the compromise solution is selected according to the TOPSIS method, with an operating cost of 395.6 yuan and an environmental cost of 216.0 yuan; when the environmental cost is taken to be the minimum value of 191.3 yuan, the corresponding operating cost is 489.1; when the operating cost takes the minimum value of 364.5 yuan, the corresponding environmental cost is 242.7 yuan, and in this paper, the compromise solution is taken to take into account the operating cost and environmental cost of the microgrid.

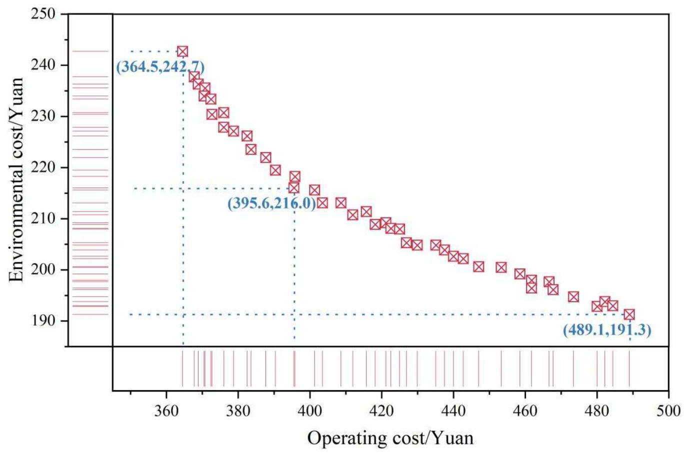

Figure 3: Microgrid multi-objective Pareto solution set

As shown in Figure 4, the dispatch result based on the iterative ADP algorithm can meet the power balance constraint in any scheduling period, where the power is positive means wind and solar output, energy storage discharge, MT output or power purchase from the distribution network, all of which belong to the situation where the microgrid obtains power, and the negative power indicates that the battery is stored and charged or sold to the distribution network.

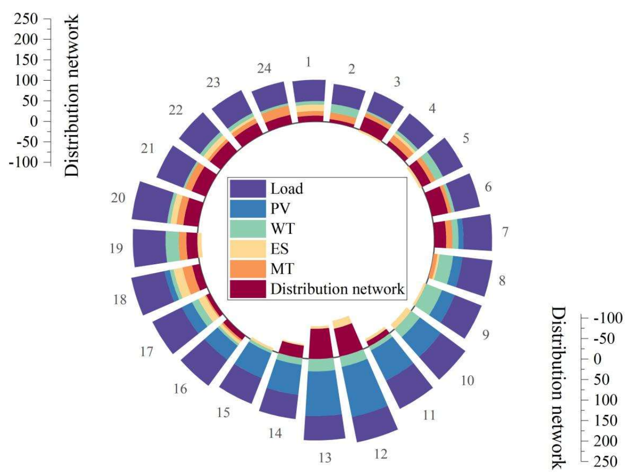

Figure 4: Output optimization results of each microgrid unit

III. B. Adaptation analysis

The microgrid unit parameters and time-of-use tariffs of the proposed grid-connected microgrid system are shown in Tables 1 and 2, respectively.

Table 1: Unit parameters

Parameter name	PV	WT	DE	MT
Power limit/kw	80	120	40	40
Lower power limit/kw	0	0	7	4
Climbing power limit/kw	0	0	2	2
Operation and maintenance unit price/(Yuan/(kW·h))	0	0	0.146	0.0308
Capacity factor	30.57	25.66	38.15	55.76
Depreciation life/year	30	20	20	25
Initial installation cost per unit capacity/(10,000 yuan/kW)	7.050	2.475	4.465	1.708

Table 2: Timesheet electricity price

Time-sharing class	Time period	Power purchase price/(Yuan/(kw·h))	Electricity price/(Yuan/(kw·h))
Peak hour	10:00~15:00	1.08	0.82
	18:00~21:00		
Mean time segment	7:00~10:00	0.64	0.58
	15:00~18:00		
	21:00~23:00		
Valley interval	23:00~7:00 the next day	0.29	0.21

In order to compare the effect of the objective function on the scheduling results, the scheduling results for different objective functions are discussed. The fitness curves when the objective functions are integrated cost, operating cost, and environmental cost are shown in Fig. 5 (a-c), respectively. From Fig. 5, it can be seen that the iterative ADP algorithm shows excellent convergence and optimization seeking ability for different objective functions set in this paper. Compared with the traditional ADP algorithm, the optimization results of the iterative ADP algorithm not only have a better diversity of particles, but also its convergence is significantly better than that of the traditional ADP, and it reaches the optimal value at the number of iterations 250, 440, and 150, respectively, when the objective function is the integrated cost, the operating cost, and the environmental cost.

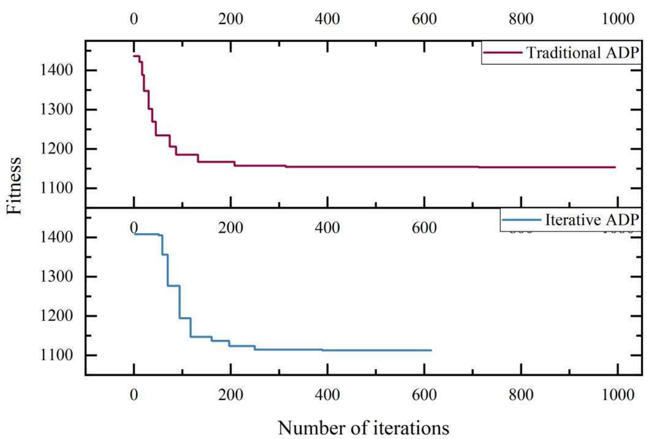

(a) Objective function-comprehensive cost

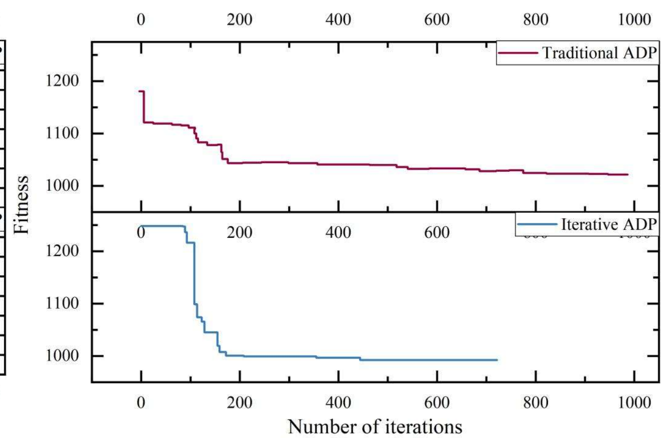

(b) Objective function-running costs

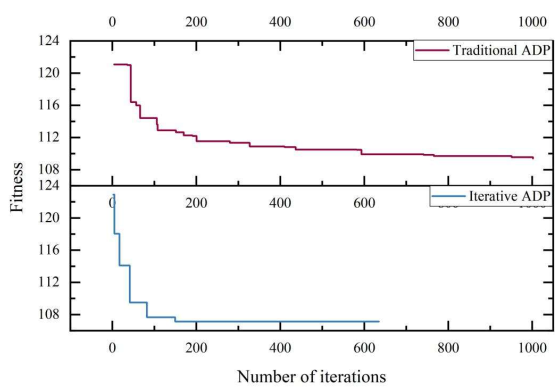

(c) Objective function-cost of pollution remediation

Figure 5: Fitness curves for different objective functions

III. C. Analysis of optimization results

The power interaction between the microgrid and the larger grid is shown in Fig. 6, and the charging and discharging of ES is shown in Fig. 7. Combined with Fig. 6 and Fig. 7, it can be seen that the PV and WT are almost in full power generation state during the scheduling cycle. From Table 2, it can be seen that, due to the lower electricity price from 23:00 to 7:00 the next day, and the lower light intensity during this time period, so the PV generates less power, in order to make up for the lack of power supply capacity, so the microgrid chooses to purchase power from the power grid, and at the same time, the ES charging is used to satisfy the supply of power during the other time periods. Between 7:00 and 10:00, the PV begins to feed power to the grid as the light intensity increases, and the microgrid's power supply capacity increases significantly, but due to the increase in load and the increase in the purchase price of power, the microgrid needs to activate the MT to meet the load's power demand, but due to the fluctuating power generation of the PV and the WT, the excess power will continue to be stored in the ES. Between 10:00 and 15:00, the microgrid sells power to the larger grid to improve the economic efficiency of the microgrid, while the ES is not recharged due to the high value of the electricity price and the sufficient power generation from PV and WT at this time. Between 15:00 and 18:00, the ES is charged because the distributed power generation in the microgrid is greater than the demand due to the decrease in electricity price and load demand. Between 18:00 and 21:00, the electricity price rises again while the load demand increases, at which time the distributed power sources in the microgrid are still generating electricity in a maximum manner and the ES starts discharging and sells the excess electricity to the larger grid to enhance the economic efficiency of the microgrid. During the period from 21:00 to 23:00, since the load and the generation power of PV, WT, etc. decrease at the same time, it is necessary to choose the power purchase and sale scheme with the big grid according to the actual situation to meet the user's power demand. From the above analysis, it can be seen that under the optimization of the iterative ADP algorithm, this microgrid achieves the desired scheme optimization results during the scheduling cycle.

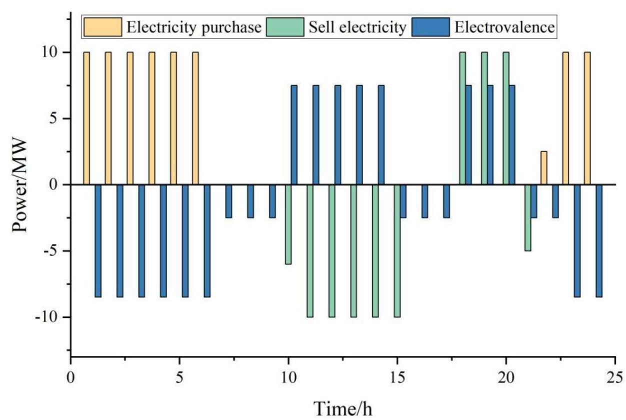

Figure 6: Interactive power between the system and the large power grid

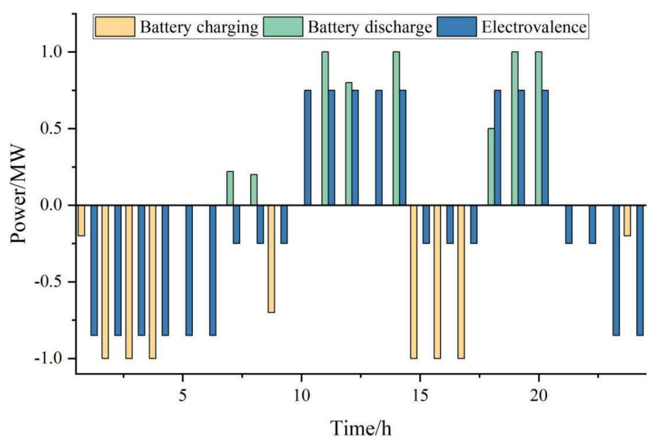

Figure 7: Energy storage optimization

IV. Conclusion

This paper focuses on the grid scheduling optimization problem under the multi-terminal information interaction architecture, and verifies the validity of the proposed model through theoretical modeling and arithmetic examples.

The proposed iterative ADP algorithm is used to solve the problem, and the compromise solution is selected according to the TOPSIS method, with an operating cost of 395.6 yuan and an environmental cost of 216.0 yuan. For different objective functions, the iterative ADP algorithm shows excellent convergence and optimization ability, compared with the traditional ADP algorithm, not only the diversity of particles is better, but also its convergence is significantly better than the optimization results of the traditional ADP, and the optimal values are reached at the number of iterations 250, 440, and 150, respectively, when the objective functions are integrated cost, running cost, and environmental cost. Simulation results show that the obtained scheduling scheme can effectively coordinate the generation power of each distributed power source.

This study provides a theoretical framework and practical paradigm for the economic-environmental cooperative scheduling of power grids under the multi-terminal interaction architecture, which can be further extended to wide-area optimization scenarios containing distributed energy clusters in the future.

Funding

This work was supported by GZKJXM20240014

References

[1] Rehmani, M. H., Reisslein, M., Rachedi, A., Erol-Kantarci, M., & Radenkovic, M. (2018). Integrating renewable energy resources into the smart grid: Recent developments in information and communication technologies. IEEE Transactions on Industrial Informatics, 14(7), 2814-2825.

[2] Ourahou, M., Ayrir, W., Hassouni, B. E., & Haddi, A. (2020). Review on smart grid control and reliability in presence of renewable energies: Challenges and prospects. Mathematics and computers in simulation, 167, 19-31.

[3] Albogamy, F. R., Paracha, M. Y. I., Hafeez, G., Khan, I., Murawwat, S., Rukh, G., ... & Khan, M. U. A. (2022). Real-time scheduling for optimal energy optimization in smart grid integrated with renewable energy sources. IEEE Access, 10, 35498-35520.

[4] Ho, W. S., Macchietto, S., Lim, J. S., Hashim, H., Muis, Z. A., & Liu, W. H. (2016). Optimal scheduling of energy storage for renewable energy distributed energy generation system. Renewable and Sustainable Energy Reviews, 58, 1100-1107.

[5] Chen, C., Wang, F., Zhou, B., Chan, K. W., Cao, Y., & Tan, Y. (2015). An interval optimization based day-ahead scheduling scheme for renewable energy management in smart distribution systems. Energy Conversion and Management, 106, 584-596.

[6] Deming, C., Pasam, P., Allam, A. R., Mohammed, R., Venkata, S. G. N., & Kothapalli, K. R. V. (2021). Real-Time Scheduling for Energy Optimization: Smart Grid Integration with Renewable Energy. Asia Pacific Journal of Energy and Environment, 8(2), 77-88.

[7] Di Somma, M., Graditi, G., Heydarian-Forushani, E., Shafie-khah, M., & Siano, P. (2018). Stochastic optimal scheduling of distributed energy resources with renewables considering economic and environmental aspects. Renewable energy, 116, 272-287.

[8] Rehman, A. U., Wadud, Z., Elavarasan, R. M., Hafeez, G., Khan, I., Shafiq, Z., & Alhelou, H. H. (2021). An optimal power usage scheduling in smart grid integrated with renewable energy sources for energy management. IEEE access, 9, 84619-84638.

[9] Alzahrani, A., Hafeez, G., Ali, S., Murawwat, S., Khan, M. I., Rehman, K., & Abed, A. M. (2023). Multi-objective energy optimization with load and distributed energy source scheduling in the smart power grid. Sustainability, 15(13), 9970.

[10] Byrne, R. H., Nguyen, T. A., Copp, D. A., Chalamala, B. R., & Gyuk, I. (2017). Energy management and optimization methods for grid energy storage systems. IEEE Access, 6, 13231-13260.

[11] Budiman, F. N., Ramli, M. A., Milyani, A. H., Bouchekara, H. R., Rawa, M., Muktiadji, R. F., & Seedahmed, M. M. (2022). Stochastic optimization for the scheduling of a grid-connected microgrid with a hybrid energy storage system considering multiple uncertainties. Energy Reports, 8, 7444-7456.

[12] Xie, P., Cai, Z., Liu, P., Li, X., Zhang, Y., & Xu, D. (2018). Microgrid system energy storage capacity optimization considering multiple time scale uncertainty coupling. IEEE Transactions on Smart Grid, 10(5), 5234-5245.

[13] Pan, C., Fan, H., Zhang, R., Sun, J., Wang, Y., & Sun, Y. (2023). An improved multi-timescale coordinated control strategy for an integrated energy system with a hybrid energy storage system. Applied Energy, 343, 121137.

[14] Wang, X., Han, L., Wang, C., Yu, H., & Yu, X. (2023). A time-scale adaptive dispatching strategy considering the matching of time characteristics and dispatching periods of the integrated energy system. Energy, 267, 126584.

[15] Abdi, H., Beigvand, S. D., & La Scala, M. (2017). A review of optimal power flow studies applied to smart grids and microgrids. Renewable and Sustainable Energy Reviews, 71, 742-766.

[16] De Carne, G., Buticchi, G., Zou, Z., & Liserre, M. (2017). Reverse power flow control in a ST-fed distribution grid. IEEE Transactions on Smart Grid, 9(4), 3811-3819.

[17] Zhang, Z., Wang, C., Chen, S., Zhao, Y., Dong, X., & Han, X. (2022). Multitime scale co-optimized dispatch for integrated electricity and natural gas system considering bidirectional interactions and renewable uncertainties. IEEE Transactions on Industry Applications, 58(4), 5317-5327.

[18] Jha, R. R., Inaolaji, A., Biswas, B. D., Suresh, A., Dubey, A., Paudyal, S., & Kamalasadan, S. (2022). Distribution grid optimal power flow (d-opf): Modeling, analysis, and benchmarking. IEEE Transactions on Power Systems, 38(4), 3654-3668.

[19] Hui, Q., Teng, Y., Zuo, H., & Chen, Z. (2019). Reactive power multi-objective optimization for multi-terminal AC/DC interconnected power systems under wind power fluctuation. CSEE Journal of Power and Energy Systems, 6(3), 630-637.

[20] Li, Z., Wei, Z., Zhan, R., Li, Y., & Zhang, X. P. (2020). System operational dispatching and scheduling strategy for hybrid cascaded multi-terminal HVDC. International Journal of Electrical Power & Energy Systems, 122, 106195.

[21] Yang, Q., Shen, J., Li, J., He, H., Wei, Z., & Igic, P. (2022). An improved adaptive coordination control of wind integrated multi-terminal HVdc system. IEEE Transactions on Power Electronics, 38(4), 5490-5499.

[22] Deng, W., Pei, W., Li, N., Zhang, G., Yi, Y., & Kong, L. (2020, June). Research on operation control technology of multi-terminal DC power distribution system based on physics/information fusion. In 2020 5th Asia Conference on Power and Electrical Engineering (ACPEE) (pp. 404-409). IEEE.

[23] Raza, A., Liu, Y., Rouzbehi, K., Jamil, M., Gilani, S. O., Dianguo, X., & Williams, B. W. (2017). Power dispatch and voltage control in multiterminal HVDC systems: A flexible approach. IEEE Access, 5, 24608-24616.